Journal of Alloys and Compounds, 213/214 (1994) 199–206
JALCOM 4029

Probing trivalent actinide ions in heavy metal fluoride glasses via laser excitation

Richard T. Brundage
St. Cloud State University, St. Cloud, MN 56301-4498 (USA)

Abstract

The demonstration of efficient fluorescence of americium and curium in heavy metal fluoride glasses opens up new possibilities for the study of the electronic structure of actinide ions. Fluorescence spectra, lifetimes and branching ratios give complementary information to absorption spectra that aids in determining energies and wavefunctions of electronic excited states as well as providing unique information on the interaction of ions and the migration of energy. Heavy metal fluoride glasses are excellent hosts for fluorescence studies, with a broad range of transparency and no high energy vibrations to compete with fluorescence via multiphonon non-radiative decay. Our studies have helped resolve the energy level structure of americium and suggest an explanation for the failure to observe laser action. Fluorescence line-narrowing experiments in curium-doped glasses allow us to estimate the ground state splitting and measure the temperature dependence of homogeneous broadening.

1. Introduction

There is renewed interest in applications of rare earths in glass, driven in part by the development of efficient semiconductor lasers at various wavelengths and low loss optical fibers [1]. Novel glasses based on zirconium and hafnium have allowed laser gain using rare earth transitions that are too weak to compete with non-radiative rates in conventional oxide glasses [2–4]. We show that these glasses can be used to study fluorescence in actinide ions as well. The lanthanides and actinides both have optical properties that are determined by transitions between f-electron states. We began a study of the actinides beyond uranium to help shed light on the properties of excited f-electron states in amorphous materials.

These studies give information complementary to previous work carried out on lanthanide systems. The larger spatial extent of the 5f orbitals compared with the 4f orbitals gives greater coupling to the lattice, putting them intermediate between the lanthanides and d-transition metals. This changes the relative strength of the interactions involved in absorption and emission of light.

We measured the effect of non-radiative decay on the fluorescence efficiency of americium in a fluorozirconate glass [5]. This work shed light on the failure to observe laser action in americium [6, 7]. We also compared observed radiative rates with those calculated using the theory of Judd [8] and Ofelt [9] and found that the theory cannot account for the observed results [10].

We observed fluorescence from curium in fluorozirconate glass as well, and studied radiative and non-radiative rates. This system does not appear to follow the prevailing model of multiphonon decay in solids [11, 12] and will require further investigation. We were able to carry out resonant fluorescence line-narrowing (FLN) experiments and set an upper limit on the ground state splitting of Cm^{3+}.

We first discuss the determination of energy levels and radiative rates. Then we consider the nature of non-radiative relaxation in actinide systems and compare them with lanthanides. We conclude with a description of the technique of FLN as applied to the measurement of the ground state splitting in Cm^{3+}.

2. Energy levels

Fluorescence is a particularly sensitive technique for the observation of weak optical transitions, because the background signal can be reduced to very low levels. The problem is that fluorescence itself can be quite weak or non-existent because of competition from other processes. As discussed in a later section, non-radiative processes can overwhelm radiative processes, particularly for weak transitions. Novel glasses have been developed that greatly reduce the strength of non-radiative processes and allow the observation of weak fluorescence transitions.

SSDI 0925-8388(93)04029-4

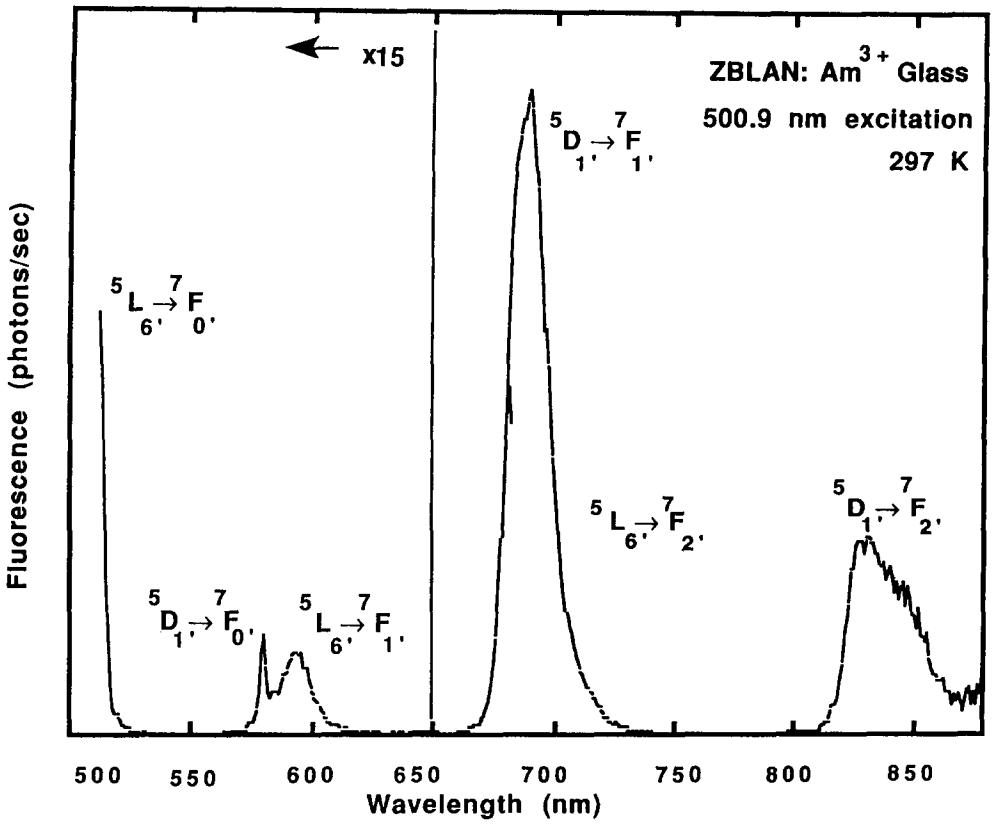

Fig. 1. Room temperature fluorescence spectrum of Am:ZBLAN glass. A color filter cuts off the spectrum for wavelengths shorter than 515 nm to block laser scatter.

Examples of such transitions are between the $^7F_0$ ground state and the $^5D_1$, $^7F_5$, $^7F_3$ and $^7F_1$ excited states of Am^{3+}. These transitions are forbidden by electric dipole selection rules, because the $J=0$ ground state has vanishing matrix elements with $J=$odd states [9]. The calculated radiative rate of 0.02 s^{-1} for the $^5D_1$ to $^7F_0$ transition is a result of magnetic dipole emission. Identification of the position of the $J=$odd states from absorption data is very difficult because of low transition rates from the $^7F_0$ ground state.

We were able to observe this transition in fluorescence from samples of fluorozirconate glass containing americium because of the low non-radiative rates in this glass. An example of a room temperature spectrum is shown in Fig. 1. Fluorescence is observed at low temperature as well. These spectra together with absorption spectra allowed us to assign energies to the $^5L_6$, $^5D_1$, $^7F_6$, $^7F_4$, $^7F_2$ and $^7F_1$ states, the latter by observation of the $^5D_1$ to $^7F_1$ fluorescence transition [13]. The energies are in good agreement with those calculated from free-ion wavefunctions.

3. Radiative rates

Am^{3+} is an interesting subject for application of the Judd–Ofelt theory of radiative rates of f–f transitions in solids. The $J=0$ ground state introduces some stringent selection rules that make evaluation of intensity parameters particularly simple. For $J=0$ to $J=$even transitions all the reduced matrix elements $(U_\lambda)_{ik}$ are zero except for $\lambda=J$. Each intensity parameter B_λ can be determined by measuring the oscillator strength of a single absorption transition. In Am^{3+} the $^7F_2$, $^7F_4$ and $^7F_6$ states are high enough in energy that transitions from the ground state lie above the IR cut-off of ZBLAN fluorozirconate glass at around 5 μm [4].

We measured these transitions in the near IR along with the visible absorption spectra, including the very pronounced absorption near 500 nm due to absorption into the $^5L_6$ state. We found that the oscillator strengths could not give a consistent set of Judd–Ofelt intensity parameters. The absorption spectrum of americium in ZBLAN glass is shown in Fig. 2. The values of Ω_6 obtained from the $^5L_6$ absorption oscillator strength, 4.3×10^{-19} cm^2, and the $^7F_6$ absorption transition, 2.3×10^{-19} cm^2, vary by nearly a factor of 2. In addition, the reduced matrix elements together with the value of Ω_4 determined from the $^7F_4$ absorption, 8.5×10^{-20} cm^2, predict absorptions at 377 and 423 nm as strong as or stronger than the $^7F_4$ absorption. These features cannot be clearly identified from the absorption spectra.

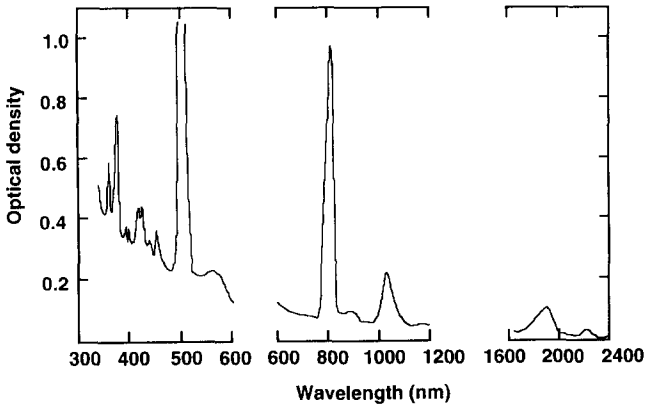

Fig. 2. Absorption spectrum of Am^{3+} in fluorozirconate glass. The spectrum is saturated at 500 nm owing to the strong $^7F_0$ to $^5L_6$ transition. The wavelength scale varies for each region of the spectrum to aid in comparing the strength of transitions, because oscillator strength is defined as the area under the absorption curve as a function of frequency.

The absorption features of curium are very weak and oscillator strengths are difficult to determine from them. An alternative method can be applied because of the special characteristics of the energy level structure of Cm^{3+}. As was pointed out by Sytsma *et al.* for Gd^{3+} [14], the large gap between the ground and the first excited state allows the determination of radiative rates for the first two excited states through measurement of the excited state lifetime and fluorescence spectra. In addition, the non-radiative decay rate of the second to the first excited state can be determined, as discussed in the following section.

The same method can be applied to Cm^{3+}, but because of the different reduced matrix elements, a complete determination of the Judd–Ofelt parameters is not possible. The first excited state in curium is the $^6D_{7/2}$ intermediate coupling state, the second is $^6D_{5/2}$. The ratio of $^6D_{5/2}$ to $^6D_{7/2}$ fluorescence is 0.034 and the fluorescence lifetime of the $^6D_{5/2}$ state is 59 μs, resulting in a calculated radiative rate of 557 s^{-1} for the $^6D_{5/2}$ state. Because radiative transitions between the $^6D_{5/2}$ and the $^8S_{7/2}$ ground state are dominated by the U_2 reduced matrix element, we are able to assign a value of 1.4×10^{-21} cm^2 for Ω_2. This is small compared with the value determined for Am^{3+} in ZBLAN, 9.2×10^{-20} cm^2 [10], but since Ω_2 is known to be quite sensitive to host and ion variation [15], this is not a surprising result.

Radiative transitions from the $^6D_{7/2}$ to the ground state involve contributions from all three intensity parameters, so neither the Ω_4 or Ω_6 parameter can be determined uniquely. The best that can be done is to put a constraint on them together. The radiative rate of $^6D_{7/2}$ is 770 s^{-1} based on the low temperature lifetime of 1.3 ms. This together with the value of Ω_2 determined from the $^6D_{5/2}$ radiative rate constrains $1.5\Omega_4+\Omega_6=8.0\times10^{-19}$ cm^2. This compares favorably with the value of 6.55×10^{-19} cm^2 from the intensity parameters found for Cm^{3+} in solution [16].

4. Non-radiative rates

Am^{3+} and Cm^{3+} are excellent candidates for fluorescence studies because both have states with large energy gaps to lower energy states. This allows light emission to compete successfully with non-radiative processes that can quench fluorescence. There is little known about the nature and strength of non-radiative processes in actinide systems.

Multiphonon emission is thought to be the dominant non-radiative process for low concentrations of ions in solids when the energy gap is larger than the highest energy phonon available from the host. A phenomenological model of multiphonon decay has been developed [11] which gives the following expression for the decay rate:

$$W_{nr}=C\exp(-a\,\Delta E)[n(\hbar\omega, T)+1]^p \quad (1)$$

where W_{nr} represents the non-radiative decay rate, ΔE is the energy gap to the next lower state, p is the number of phonons required for that transition and the two parameters C and a are characteristic of the material. The Bose–Einstein distribution $n(\hbar\omega, T)$ is evaluated for phonons of energy $\hbar\omega=\Delta E/p$ at temperature T.

This expression gives an accurate representation for multiphonon decay in both crystals and glasses containing rare earth ions [17]. We have applied it to the study of the temperature dependence of the fluorescence spectra and lifetimes of excited states of americium and curium in fluorozirconate glass. The observed behavior of Am^{3+} agrees well with the predictions of theory, while the dynamics of Cm^{3+} fluorescence does not.

Non-radiative rates can be determined easily from the total decay rate if the radiative rate is known. It is common to apply the Judd–Ofelt theory to the calculation of radiative rates and measure total decay rates through the fluorescence decay time. In the case of Am^{3+} in ZBLAN glass, as discussed above, the Judd–Ofelt theory gives conflicting results, so another method was used to determine the radiative rate. The method of determining radiative rates in Cm^{3+} gives the non-radiative rate of the $^6D_{5/2}$ state at the same time.

In principle, the Einstein A and B coefficients of a transition can be used to determine radiative rates from absorption oscillator strengths. In practice, one must also take into account the effect of the thermal population of crystal field components. This also changes

the fluorescence spectrum with varying temperature. McCumber [18] and others [19, 20] have developed theories to account for this effect in both the radiative rate and fluorescence spectrum.

This has allowed us to reproduce the variation in the $^5L_6$ to $^7F_0$ fluorescence with temperature, which is shown in Fig. 3, and also to calculate the radiative rate. This together with the fluorescence lifetime and the branching ratio of the fluorescence to the ground state allows us to determine the non-radiative rate as a function of temperature [5]. The calculated non-radiative, radiative and total decay rates are plotted in Fig. 4 along with the temperature dependence of the non-radiative rate predicted by the multiphonon decay model. The calculated low temperature non-radiative rate of 63 000 s^{-1} is significantly larger than the value of 48 000 s^{-1} predicted for a rare earth ion in a similar glass [21], reflecting the greater coupling of actinide ions to the host compared with lanthanides.

These results shed light on the failure to observe laser action in americium. Although the $^5L_6$ state has a large oscillator strength in absorption, much of this is not available for gain by stimulated emission, because the crystal field levels responsible are not populated at reasonable temperatures. It is a coincidence that the non-radiative and radiative rates at room temperature result in a fluorescence lifetime of about 10 μs that is near the 60 μs value predicted from the application of the simple Einstein A and B formalism to the absorption spectrum. The quantum efficiency of the $^5L_6$ emission is actually quite small and, though it does increase with temperature because the radiative rate increases faster than the non-radiative rate, it will not become large enough for laser operation.

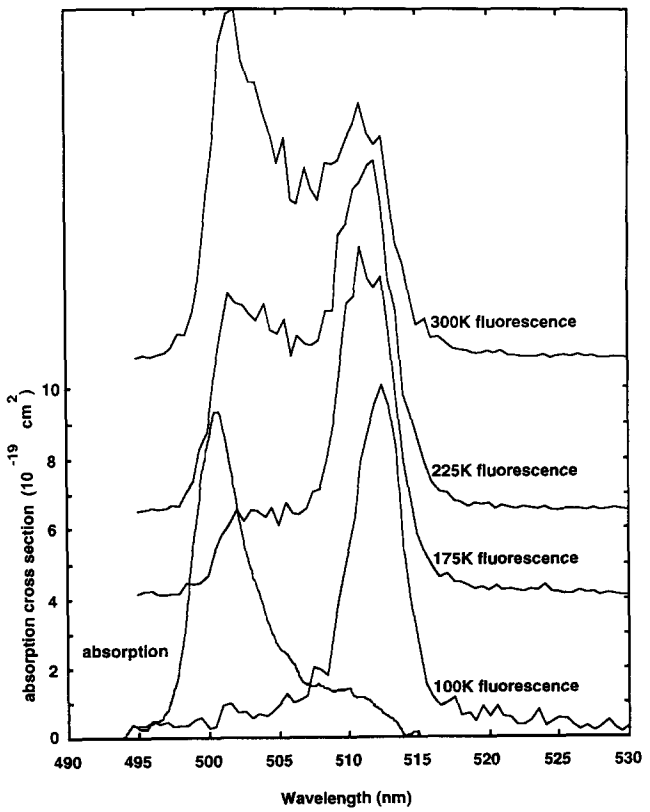

Fig. 3. Absorption and temperature-dependent emission spectra of the $^5L_6$ to $^7F_0$ transition of Am^{3+} in fluorozirconate glass.

Multiphonon decay does not explain, however, the reduction in lifetime observed for the $^5D_1$ state in higher concentration glass samples [22] or the variation with temperature reported for americium in thorium dioxide powders [23]. Beitz and Brundage [22] reported a lifetime of 0.53 ms at room temperature for the $^5D_1$ state of Am^{3+} in ZBLAN with a concentration of 7.5×10^{19} cm^{-3}. This is about a factor of 2 less than that observed for a low concentration sample, 1.7×10^{18} cm^{-3}, at room temperature. This suggests that a concentration-dependent effect is responsible for the change.

The temperature dependence of the non-radiative rate predicted by the multiphonon model also suggests that there must be another source for the reduction in lifetime. The energy gap to the next lowest level, the $^7F_6$ state, is about 4740 cm^{-1}. The low temperature rate would have to be around 400 s^{-1} to account for the observed room temperature lifetime. The low temperature rate of 63 000 s^{-1} determined for the $^5L_6$ state with an energy gap of 2230 cm^{-1} means that the coefficient a in eqn. (1) would have to be around 0.06 cm, compared with a value of 0.0058 cm observed for erbium in fluorozirconate glass. This factor-of-10 difference in the exponential energy gap dependence would mean actinides are much less sensitive to the energy difference between states. This would result in radiative transitions from states with lower energy gaps than the 2230 cm^{-1} of $^5L_6$; such transitions are not observed.

Hubert and Thouvenot [23] reported a change in lifetime for the $^5D_1$ state of americium in ThO_2 from 870 μs at 10 K to 420 μs at 300 K. The largest phonons available in ThO_2 have an energy of 575 cm^{-1}. Their phonon occupation number changes from zero at 10 K to about 0.06 at room temperature. It takes 8.7 of these phonons to bridge the 5000 cm^{-1} gap between $^5D_1$ and $^7F_6$ in ThO_2. With these parameters, eqn. (1) predicts a ratio of non-radiative rates at 300 and 10 K of 1.66.

This cannot be made consistent with the observed lifetime variation for a constant positive value of the radiative rate. The observed change in decay rate is greater than can be accounted for by the multiphonon model. One must invoke either a variation in radiative rate with temperature or additional non-radiative processes with stronger temperature dependences than multiphonon decay.

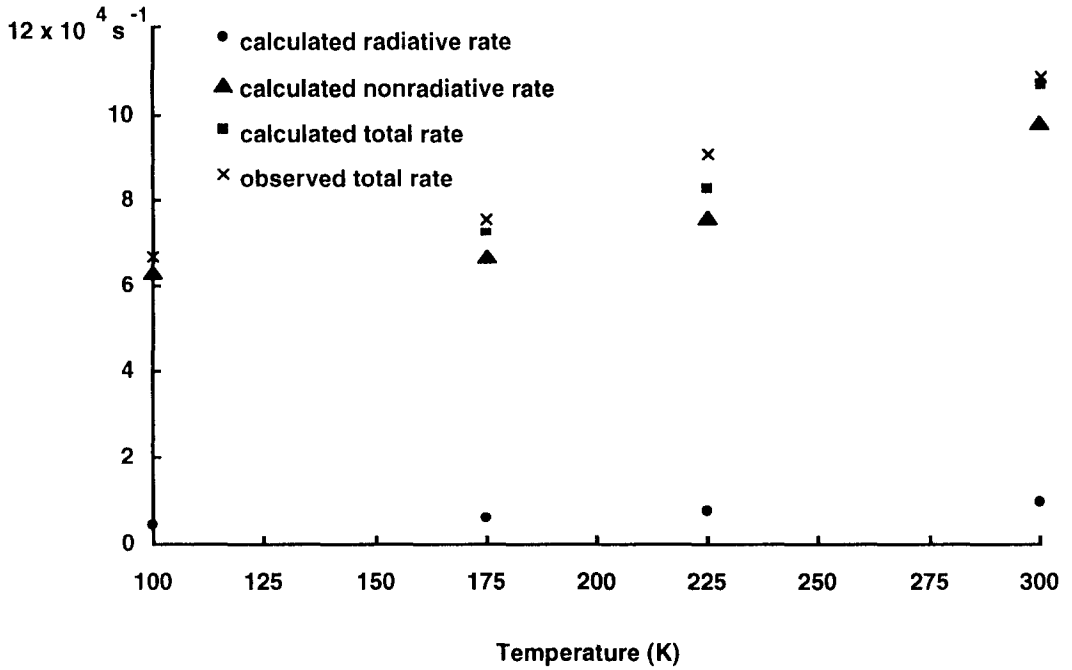

Fig. 4. Non-radiative, radiative and total decay rates as a function of temperature for Am^{3+} in fluorozirconate glass. The predicted multiphonon rate curve is derived from eqn. (1) and the observed low temperature rate.

Radiative rates can acquire temperature dependence through the population of excited state crystal field levels with larger decay rates or through phonon-assisted radiative transitions [24]. The former is responsible for the change in the fluorescence spectrum and radiative decay rate of the $^5L_6$ state discussed earlier. Some change in the relative strength of crystal field components is observed in the Am:ThO_2 spectrum. Vibronic sidebands are not observed in the fluorescence spectrum at 10 K but appear at 300 K. It is difficult at present to determine which if either of these effects is large enough to account for the change in decay rate.

Other possible non-radiative processes that could account for the change in lifetime involve energy transfer to defects sites [25, 26]. Such processes can be strongly temperature dependent but usually result in non-exponential decay with time, contrary to the observed decay in Am:ThO_2. One would also expect a concentration dependence of the non-radiative decay rate if the energy transfer process involved steps between americium ions. Fluorescence decay data were reported for only one concentration, so this interpretation of the change in decay rate with temperature will require further investigation.

We explored the decay rate of curium in fluorozirconate glass *vs.* temperature and concentration by the method mentioned earlier in determination of the Judd–Ofelt intensity parameters. Figure 5 shows the observed decay rate for two samples along with the predicted temperature dependence from the multiphonon model. It is clear that, similarly to the case of the $^5D_1$ state of americium in ThO_2, the temperature dependence predicted by the multiphonon model is not large enough to explain the observations. In addition, the non-radiative rate is greater for the low concentration sample than for the high concentration sample, which is the reverse of what would be expected for energy transfer processes involving curium-to-curium transfer. Further investigation will be required to resolve this paradox.

5. Homogeneous linewidths and ground state splitting in Cm^{3+}

Cm^{3+} has a very small ground state splitting because of selection rules introduced by the half-filled f-electron shell [27]. In glass, this splitting is obscured by the inhomogeneous broadening that arises from the site-to-site variation in the strength and symmetry of the crystal field. Selective excitation of a subset of ions by a narrowband laser can reveal the underlying structure, because the fluorescence will be characteristic of a subset of ions with a linewidth limited by either the laser or the coherence time of the excited state [28].

Two such laser techniques that have been successfully applied to lanthanide ions in glasses are spectral hole burning (SHB) [29] and fluorescence line narrowing (FLN) [30]. FLN [31, 32] and SHB [33, 34] have been used in actinide-doped crystals, but we are unaware of previous application to actinide-doped glasses. We present preliminary results of FLN experiments carried

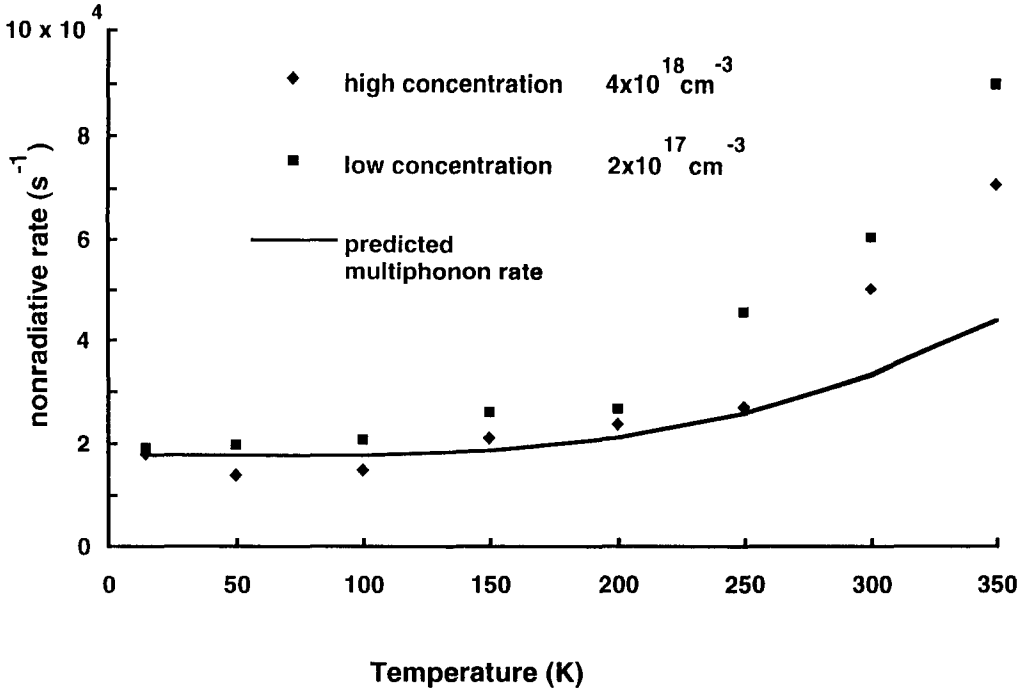

Fig. 5. Non-radiative rates as a function of temperature for Cm^{3+} in fluorozirconate glass. The predicted multiphonon rate curve is derived from eqn. (1) and the observed low temperature rate.

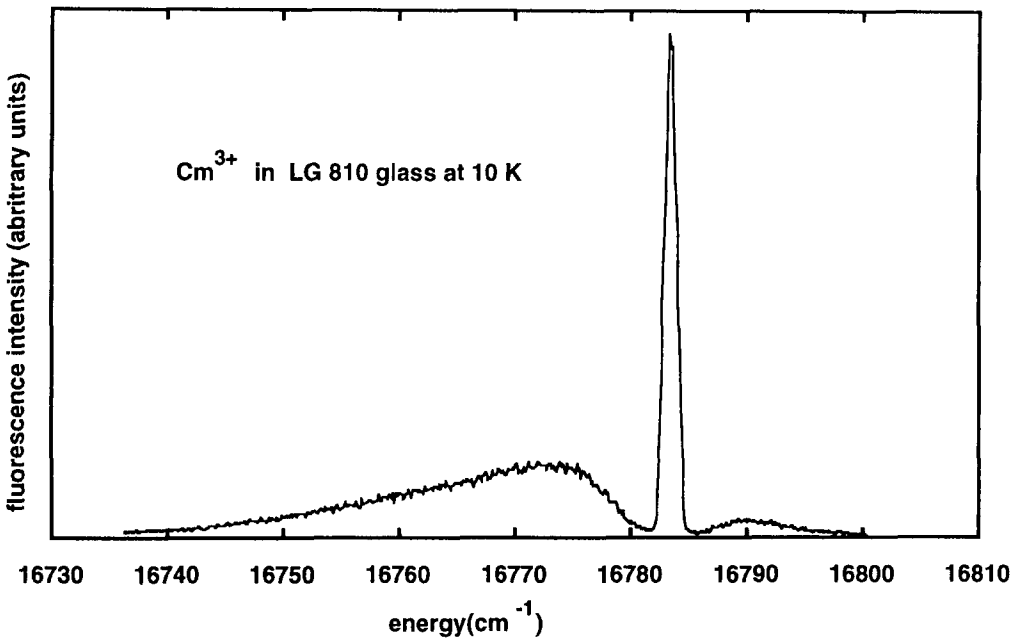

Fig. 6. Low temperature fluorescence spectrum of Cm^{3+} in LG 810 glass.

out on Cm^{3+} in ZBLAN and a fluorophosphate glass (Schott LG 810) [35].

One difficulty with FLN is the problem of accidental degeneracy. If the fluorescence transition monitored is not the same as the excitation transition, the observed fluorescence may not be fully narrowed. Ions that have the same energy for two states do not necessarily have the same energy for a third. The problem is that observing at the excitation wavelength requires a fast shutter to prevent saturation or even damage to the detection electronics by the strong scattered laser signal. We used a mechanical shutter to block the detector and an acousto-optic modulator to switch on and off a continuous wave dye laser (Coherent 899).

ground state crystal field components. Because the excited state inhomogeneous width for one crystal field level is larger than the ground state splitting of these four levels, there is a set of sites for each crystal field level such that the laser causes transitions between that particular level and the lowest level of the excited state. Thus the laser excites four groups of sites, each characterized by the crystal field level that the excitation originated from. These groups will not have equal populations because of the Boltzmann distribution among the ground state components.

The narrow feature in the fluorescence spectrum is the sum of four transitions, where each group returns to the crystal field component in the ground state it originated from. The widths of these transitions are limited by the coherence of the excited state, because the same states are involved in both excitation and emission. The other 12 transitions will suffer from accidental degeneracy as outlined above and are responsible for the broad background.

The asymmetry of the background is a result of the thermal distribution among the different crystal field levels. Transitions involving the lowest crystal field level group will result in fluorescence with energy equal to or less than the sharp line, while transitions from the highest crystal field level group will have energies equal to or greater than the sharp component.

We can estimate the total crystal field splitting between the lowest and highest crystal field components from the energy difference between the sharp component and the low energy edge of the broad component. The spectrum indicates that the total crystal field splitting of the ground state is less than 50 cm^{-1}. A more stringent limit on crystal field splitting should be possible through more detailed analysis of the fluorescence. This limit is substantially larger than the value of splitting found in $LaCl_3$ (1.97 cm^{-1}) [32].

As the temperature is increased, the width of the sharp feature increases owing to a loss of coherence of the excited state. There has been considerable work devoted to explanation of the temperature dependence of the homogeneous linewidth of lanthanide ions in glasses, which is significantly different from that of crystals [36]. A common feature of these studies is the observation of linewidths proportional to T^2 above 30 K.

We have measured the temperature dependence of the homogeneous width of the $^6D_{7/2}$ to $^8S_{7/2}$ transition between 35 and 100 K in ZBLAN and LG 810 glass. The results are consistent with a power-law dependence of T^2, while the magnitude of the broadening is intermediate between that observed in Nd [37] and Eu [38]. This is surprising, because one would assume the larger coupling to the lattice of the actinides would result in larger linewidths. More detailed analysis of this problem will be presented in a later paper.

Acknowledgments

Preparation of glass samples and FLN studies were carried out at the Argonne National Laboratory. The FLN studies were carried out in collaboration with G.K. Liu and James V. Beitz. This work was supported by the National Science Foundation grant DMR 881 3333 and the division of Educational Programs at Argonne.

References

1 P. Urquhart, *Proc. IEEE, 135* (1988) 385.
2 R.M. Almeida (ed.), *NATO ADI Series E, Applied Sciences,* Vol. 123, *Halide Glasses for Infrared Fiberoptics,* Martinus Nijhoff, Dordrecht, 1987.
3 P.W. France, *Fluoride Glass Optical Fibres,* Blackie, Edinburgh, 1990.
4 M.G. Drexhage, Heavy metal fluoride glasses, in M. Tomozawa and R.H. Doremus (eds.), *Glass IV,* Academic, New York, 1985, p. 151.
5 M.C. Williams and R.T. Brundage, *Phys. Rev. B, 45* (1992) 4561.
6 H.A. Friedman and J.T. Bell, *J. Inorg. Nucl. Chem., 34* (1972) 3928.
7 B. Finch and G.W. Clark, *J. Phys. Chem. Solids, 34* (1973) 922.
8 B.R. Judd, *Phys. Rev., 127* (1962) 750.
9 G.S. Ofelt, *J. Chem. Phys., 37* (1962) 511.
10 R.T. Brundage, M.M. Svatos and R. Grinbergs, *J. Chem. Phys., 95* (1991) 7933.
11 C.B. Layne, W.H. Lowdermilk and M.J. Weber, *Phys. Rev. B, 16* (1977) 10.
12 W.H. Fonger and C.W. Struck, *J. Luminesc., 17* (1978) 241.
13 R.W. Valenzuela and R.T. Brundage, *J. Chem. Phys., 93* (1990) 8469.
14 J. Sytsma, G.F. Imbusch and G. Blasse, *J. Chem. Phys., 91* (1989) 1456.
15 W.T. Carnall, H. Crosswhite and K. Rajnak, A systematic view of transition intensities in the spectra of actinides and lanthanides in condensed phases, in B. Jezowska-Trebiatowska, J. Legendziewica and W. Strek (eds.), *Proc. Int. Symp. on Rare Earths Spectroscopy,* World Scientific, Singapore, 1985, p. 267.
16 W.T. Carnall and K. Rajnak, *J. Chem. Phys., 63* (1975) 3510.
17 M.F.H. Schuurmans and J.M.F. v. Dijk, *Physica B, 123* (1984) 131.
18 D.E. McCumber, *Phys. Rev., 134* (1964) A299.
19 B.S. Neporent, *Sov. Phys. – Dokl., 3* (1958) 337.
20 Y.B. Band and D.F. Heller, *Phys. Rev. A, 38* (1988) 1885.
21 M.D. Shinn, W.A. Sibley, M.G. Drexhage and R.N. Brown, *Phys. Rev. B, 27* (1983) 6635.
22 J.V. Beitz and R.T. Brundage, *J. Alloys Comp., 181* (1991) 49.
23 S. Hubert and P. Thouvenot, *J. Luminesc., 54* (1992) 103.
24 T. Miyakawa and D.L. Dexter, *Phys. Rev. B, 1* (1970) 2961.

25 R.T. Brundage, Optical energy transfer in activated glasses, in W.M. Yen (ed.), *Dynamical Processes in Disordered Materials,* Trans Tech, Zürich, 1989, p. 139.
26 T.T. Basiev, V.A. Malyshev and A.K. Przhevuskii, Spectral migration of excitations in rare-earth activated glasses, in A.A. Kaplyanskii and R.M. Macfarlane (eds.), *Spectroscopy of Solids Containing Rare Earth Ions,* Elsevier, New York, 1987, p. 275.
27 B.G. Wybourne, *Phys. Rev., 148* (1966) 317.
28 M.J. Weber, Laser excited fluorescence spectroscopy in glass, in W.M. Yen and P.M. Selzer (eds.), *Laser Spectroscopy of Solids,* Springer, Berlin, 1981, p. 189.
29 R.M. Macfarlane and R.M. Shelby, *Opt. Commun., 45* (1983) 46.
30 W.M. Yen and R.T. Brundage, *J. Luminesc., 36* (1987) 209.
31 J.P. Hessler, R.T. Brundage, J. Hegarty and W.M. Yen, *Opt. Lett., 5* (1980) 348.
32 G.K. Liu and J.V. Beitz, *J. Chem. Phys., 99* (1993) 3304.
33 K. Holliday and N.B. Manson, *J. Phys.: Condens. Matter, 1* (1989) 1339.
34 G.K. Liu and J.V. Beitz, *Chem. Phys. Lett., 171* (1990) 335.
35 L. Cook and K.-H. Mader, *J. Am. Ceram. Soc., 65* (1982) 579.
36 R.M. Macfarlane and R.M. Shelby, *J. Luminesc., 36* (1987) 179.
37 J.M. Pellegrino, W.M. Yen and M.J. Weber, *J. Appl. Phys., 51* (1980) 6332.
38 F. Durville, G.S. Dixon and R.C. Powell, *J. Luminesc., 36* (1987) 221.